Nuclear energy level complexity: Fano factor signature of chaotic behavior of nearest-neighbor time-series analysis

Diego Alberto Lara Bustillos,[1] Leonardo López-Hernández,[1] N. Ramírez-Cruz,[1] Edna M. Hernández,[1,*] Ruben Fossion,[2,3] Enrique López-Moreno,[1] Carlos E. Vargas,[4] and V. Velázquez[1]

[1]*Facultad de Ciencias, Universidad Nacional Autónoma de México, Apartado Postal 70-543, 04510 México, Distrito Federal, México*

[2]*Instituto de Ciencias Nucleares, Universidad Nacional Autónoma de México, Apartado Postal 70-543, 04510 México, Distrito Federal, México*

[3]*Centro de Ciencias de la Complejidad (C3), Universidad Nacional Autónoma de México, Apartado Postal 70-543, 04510 México, Distrito Federal, México*

[4]*Facultad de Física, Universidad Veracruzana, CP 91000 Xalapa, Veracruz, México*

(Received 22 January 2018; accepted 19 August 2020; published 1 October 2020)

Background: The Fano factor is used to characterize statistical noises, in quantum optics to determine correlations and anticorrelations, in transport theory to characterize the limit of quantum chaos experienced by electrons in a mesoscopic cavity. However, to our knowledge, it has not been used in nuclear physics to study the spectral fluctuations.

Purpose: In the present contribution, we applied the square root of the Fano factor ($\hat{f}$) to random matrix theory and to the energy level statistics of the nuclear excitation spectrum to determine if the Fano factor can be used to study nuclear energy spectra distributions.

Methods: We studied the fluctuation of the excited states of ^{48}Ca, ^{48}Ti, and ^{46}Ti with symmetry $J^P = 3^+$ as well as the Wigner distribution and the Fourier power spectrum of the energy level spacings for different quadrupole interactions so we can determine when we have a chaotic distribution. Later on we compared with the Fano factor of the same distributions.

Results: The Fano factor agrees with that obtained by the other methods. We show that $\hat{f} = 0.5$ corresponds to quantum chaos for the energy levels in the nuclear spectra.

Conclusions: The Fano factor can be used in nuclear physics (and other areas of science) to determine quantum chaos.

DOI: 10.1103/PhysRevC.102.044301

I. INTRODUCTION

Our limited capacities on the prediction of complex dynamic systems have led us to study the behavior of their fluctuations in order to obtain more information about their complexity. In the last century several methods have been developed to classify and determine them, such as the Fano factor, the second-order correlation function, the Wigner distribution, and the Fourier power spectrum, for example. Using these methods the fluctuations can be classified as the well known Brown noise, Poisson noise, or chaotic noise. It is important to remark that limitations inherent to each method have made it difficult to study the types of noises with more than one or two methods. In particular, the quantum chaotic noise of nuclear spectra has been studied by the Wigner distribution [1–4], by the random matrix theory (RMT) [5–8], and, most recently, by the Fourier power spectrum [9–11]. Here we will explore if the Fano factor can be used also to study quantum chaotic noise of nuclear spectra.

The Fano factor [12,13], defined as the ratio of the variance to the average number of events in a defined time interval, is normally used to study the correlation of identical events that come from certain types of phenomena. Using this method the fluctuations can be classified as correlated, uncorrelated, and anticorrelated, which correspond to super-Poissonian, Poissonian, and sub-Poissonian noises, respectively. The noise associated to the appearance of individual uncorrelated events is known as shot noise [14]. The magnitude of this noise grows above the shot noise for correlated events and decreases below the shot noise for anticorrelated events. The value of the Fano factor is $F = 1$ for shot noise and $F = 2$ for twin uncorrelated events. An example of twin uncorrelated events are the statistics associated to the detection of pairs of particles (electrons or photons) appearing randomly. The absence of noise is given by $F = 0$, which indicates that identical events in the particle number always appear at the same time interval, i.e., with a perfect anticorrelation.

The Fano factor has been used in several areas of science such as the study of electrical spikes in neuronal activity [15,16], spanning of earthquakes [17], and chemical reactions [18], among other applications. Additionally, it has been widely used in quantum optics, where the square root of the

*ednah@ciencias.unam.mx

Fano factor is applied [19] to characterize the type of photon source through the fluctuations in the average number of photons, $\bar{n}$:

$$\hat{f} = \frac{\sigma_n}{\sqrt{\bar{n}}}, \tag{1}$$

where σ_n is the root mean square. It is well known that $\hat{f}_P = 1$ for series that follow Poisson distribution, such as laser time series and $0 \leqslant \hat{f}_Q < 1$ for nearly identical events, like quantum light source time series. The Fano factor has been also used to study quantum chaos. The first studies that relate a distinct value of the Fano factor with quantum chaos were performed on the electronic transport theory in mesoscopic cavities [20–25], where it was established that quantum chaos corresponds to $F = 1/4$. To our knowledge, the Fano factor has not been used to study the fluctuations of nuclear energy level spacings.

In this article we show that the Fano factor can be used as a criterion to determine quantum chaos statistics in atomic nuclei. We will show that a signature of quantum chaos in the cases of ^{46}Ti, ^{48}Ti, and ^{48}Ca is $\hat{f}_Q \approx 1/2$, in agreement with ballistic billiards theory. In fact we use the most simple form of the Fano factor shown in Eq. (1).

The organization of this article is the following: We obtain the energy spectra for ^{46}Ti, ^{48}Ti, and ^{48}Ca, then we apply the Wigner and Poisson surmises to the fluctuations of nuclear energy level spacings for nearest-neighbors. In the next section, we make a similar analysis using the Fourier power spectrum method. Finally we apply the Fano factor and we compare the three methods for the description of quantum chaos in order to outline the efficacy of the Fano factor method.

II. NUCLEAR ENERGY LEVELS AND THE WIGNER SURMISE

Here we studied the fluctuations of the excited states of ^{48}Ca, ^{48}Ti, and ^{46}Ti with symmetry $J^P = 3^+$ using the shell model calculation [26,27] in the full pf shell. This was achieved using the schematic Hamiltonian

$$\hat{H}_{SM} = \hat{H}_m - \chi \hat{Q} \cdot \hat{Q} + g_P \hat{P} \cdot \hat{P}, \tag{2}$$

which contains a monopolar field ($\hat{H}_m$) [28,29] and two 2-body interactions, one of a pairing type ($\hat{P}$) and another of a quadrupole type ($\hat{Q}$). The pairing interaction was applied with a coefficient $g_P \approx 0.45$, whereas the quadrupole interaction was modulated by a parameter χ, which can be modified to span the limits of Poisson and chaotic statistics.

Figure 1 shows the results for the diagonalization corresponding to a transition in the quadrupole interaction from $\chi = 0.005$ to 0.25 for ^{46}Ti, ^{48}Ti, and ^{48}Ca.

The individual energy sequences E_i were unfolded, in such a way that the system-dependent global trend is excluded and only the local fluctuations ϵ_i around the average trend are retained [30]. Then, the normalized energy level spacings were calculated, $s_i = \epsilon_{i+1} - \epsilon_i$, with $i = 1, \ldots, N-1$, and the distribution $P(s)$ of these normalized energy level spacings was obtained for different values of the quadrupole-quadrupole interaction χ. It is important to note that ^{48}Ca has very well

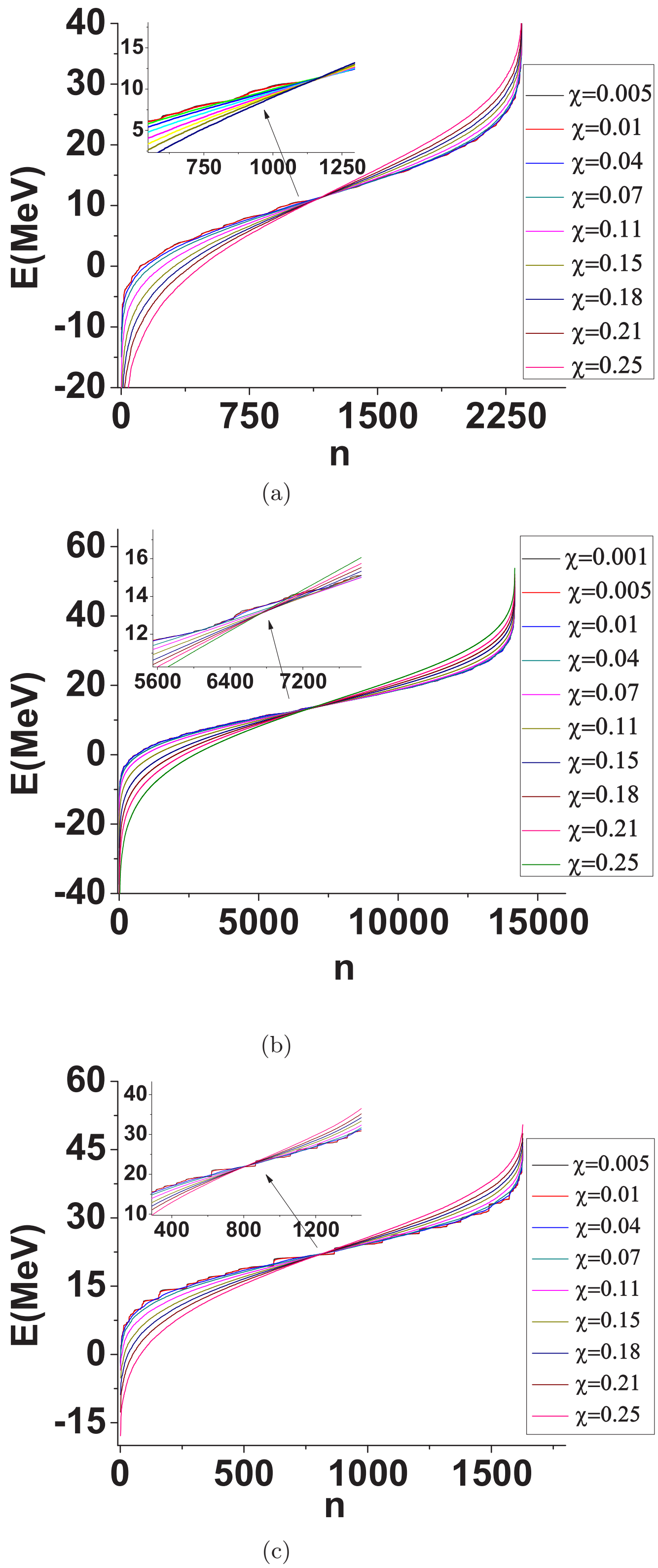

FIG. 1. Eigenvalue sequence E_i as function of the number of states for (a) ^{46}Ti, (b) ^{48}Ti, and (c) ^{48}Ca with $J = 3$ for different quadrupole strengths (χ). Discontinuous jumps in the energy sequences are found for weak interactions, but seem more intense in ^{48}Ca.

defined jumps for weak interactions [see the inset in Fig. 1(c)]. This behavior is perceptible for $^{46-48}$Ti [insets in Figs. 1(a) and 1(b)]. The jumping behavior in the energy distribution comes from a bunching effect of the energy levels that we will discuss later.

In Fig. 2 we show the nearest-neighbor distributions $P(s)$ as function of the energy level spacing s for different quadrupole-quadrupole interactions for (a) ^{46}Ti, (b) ^{48}Ti, and (c) ^{48}Ca. In this figure we can see clearly that the behavior of $P(s)$ for values $\chi < 0.01$ in the three nuclei agrees best with the Poisson distribution, whereas $P(s)$ behavior for $\chi > 0.01$ agrees with the Wigner distribution for the ^{48}Ca nucleus. However, for $^{46-48}$Ti, the statistics seem to be in the middle, i.e., between Poisson and Wigner distributions. In particular for ^{46}Ti the distribution approximates more closely the Poisson distribution than the Wigner distribution for all interactions when compared with ^{48}Ti. This indicates that the number of valence nucleons affects the distribution $P(s)$. Furthermore, when comparing ^{48}Ti with ^{48}Ca we observe that the interplay between proton and neutron shells, and even between shells of the same isospin number, also modifies the distributions of the energy level spacing.

III. THE FOURIER POWER SPECTRUM (PS) METHOD

We obtained the fluctuations of the nuclear energy spectra by considering the time series $\sum_{i=1}^{n}(s_i - \langle s\rangle) = \sum_{i=1}^{n} w_i$, where the quantity w_i represents the fluctuations of the ith spacing s_i from its mean value $\langle s\rangle$ and where the order number $n = 1, \ldots, N-1$ takes the place of time. Following this line of thought [9], we calculated its Fourier transform. If the system follows a power law, there exists a relationship between the density of frequencies and the power β: PS $= 1/f^{\beta}$, where f is the frequency. The classical limit (Poisson distribution) and the chaotic limit (Wigner distribution) correspond to $\beta = 2$ and $\beta = 1$, respectively.

Figure 3 shows the power β as function of the χ parameter of the $\hat{Q}\cdot\hat{Q}$ interaction, for the three nuclei in consideration. The results are very similar to the previous conclusions for the statistics of nearest-neighbor energy level spacings. For weak interactions all nuclei follow the Poisson distribution, but for high interactions there are several differences. The Fourier power spectrum of ^{48}Ca is closer to $1/f$ noise, while ^{46}Ti and ^{48}Ti are closer to $1/f^2$. However, ^{48}Ti has a faster transition from $\beta = 2.2$ to $\beta \approx 1.3$. Furthermore, the β for ^{48}Ti is closer to chaotic behavior than Poisson for high $\hat{Q}\cdot\hat{Q}$ interactions, while the β for ^{46}Ti for the same values is closer to Poisson behavior than chaotic. It is also important to note that ^{48}Ti drops to Poisson behavior faster than ^{48}Ca. In general, the information obtained from the nearest-neighbor distribution method is confirmed by the PS method.

All results till now indicate we have nuclear systems composed by nucleons filling energy levels following the rules of the harmonic oscillator with the corresponding degrees of degeneration. The degeneration is broken for two kind of interactions, for one and two bodies. These interactions produce repulsion among levels; then if these interactions are strong enough, neighboring levels are repelled. This is different between Poisson and Wigner, because the Poisson distribution corresponds to $1/f^2$, while Wigner corresponds to $1/f$ noises, respectively.

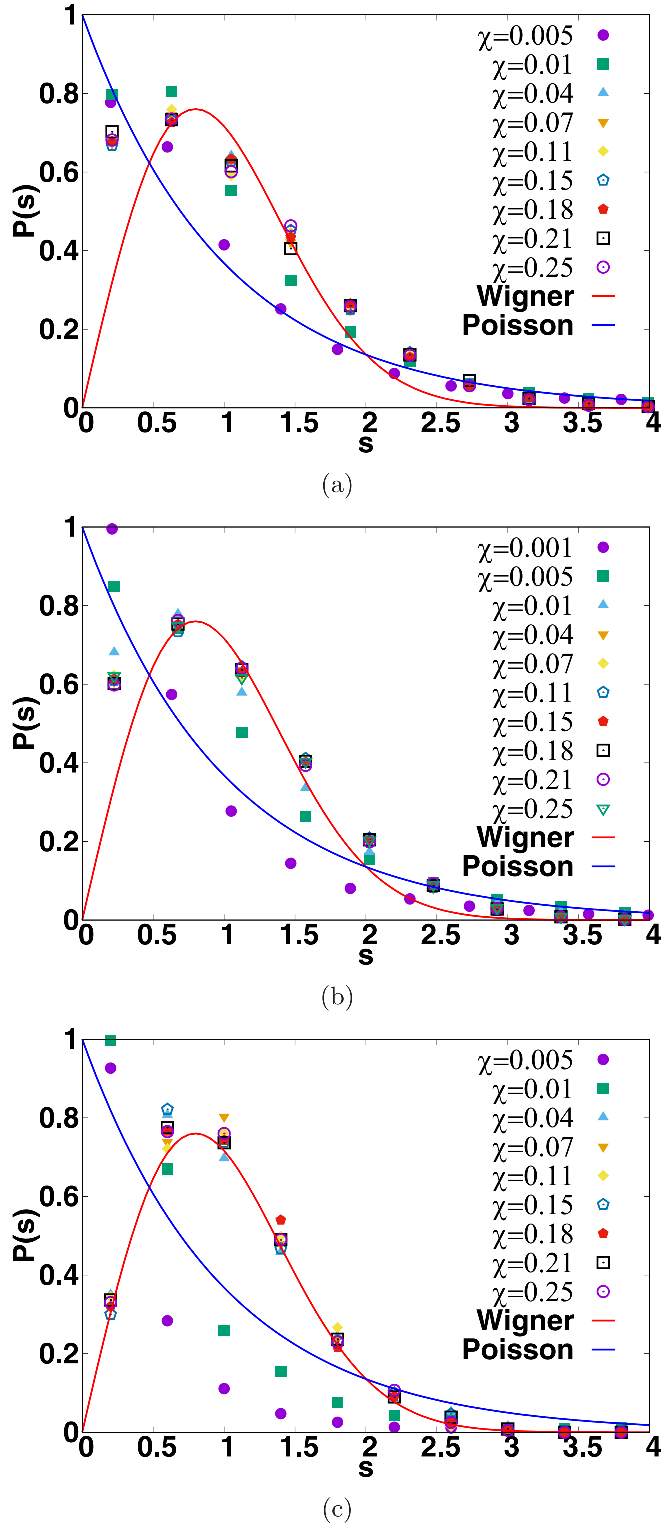

FIG. 2. Nearest-neighbor distributions $P(s)$ as function of the energy level spacings s_i for different quadrupole interactions χ, for (a) ^{46}Ti, (b) ^{48}Ti, and (c) ^{48}Ca. Only ^{48}Ca fits very well the Wigner surmise.

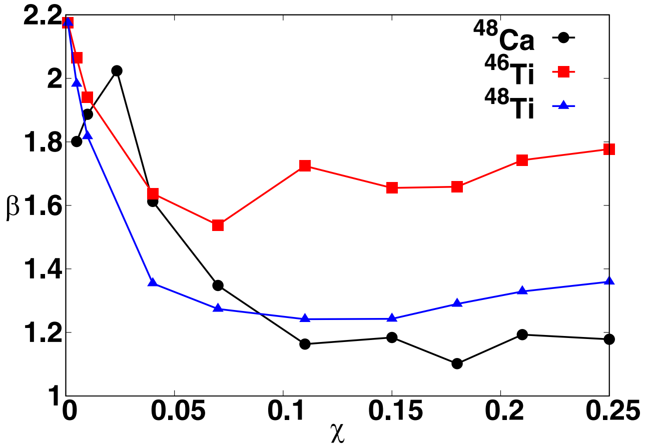

FIG. 3. Fourier power spectrum analysis for ^{48}Ca, ^{48}Ti, and ^{46}Ti as function of the intensity χ of the $\hat{Q}\cdot\hat{Q}$ interaction.

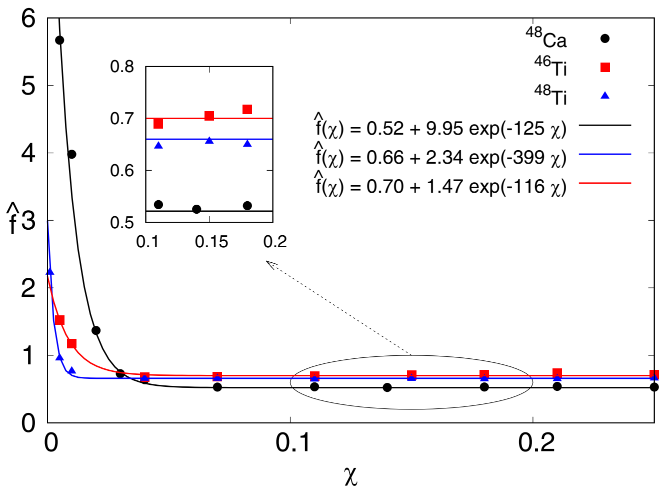

FIG. 4. Fano factor $\hat{f}$ as function of the quadrupole intensity χ for the the three nuclei $^{46\text{–}48}$Ti and ^{48}Ca.

IV. FANO FACTOR

We also calculated the square root of the Fano factor $\hat{f} = \sigma_s/\sqrt{\bar{s}}$ for the unfolded nuclear energy levels, for different quadrupole-quadrupole interactions. In Fig. 4 we show $\hat{f}$ as function of the intensity χ. For $\chi \geqslant 0.04$ the Fano factor of ^{48}Ca is $\hat{f} = 0.52 \pm 0.04$, whereas the Fano factor is $\hat{f} = 0.67$ and $\hat{f} = 0.7$ for ^{48}Ti and ^{46}Ti, respectively, with similar uncertainties. As we stated before, $\hat{f} = \sqrt{F} = 1/2$ corresponds to quantum chaos. Therefore, the ^{48}Ca behavior for large values of χ is closer to quantum chaotic behavior than ^{48}Ti and ^{46}Ti behaviors. These results imply consistency between the different methods: nearest-neighbor energy level distribution, the Fourier power spectrum, and the Fano factor.

The behavior of the Fano factor for $\chi \leqslant 0.04$ shows a statistic transition for each nucleus. $^{46\text{–}48}$Ti start from $\hat{f} = 2$ for $\chi \approx 0.01$, which means the presence of energy level bunching or the remainder of the broken quantum oscillator energy degeneration. In these terms, for weak interactions ^{48}Ca presents a larger energy level bunching than $^{46\text{–}48}$Ti.

With the objective to complete the generalization of the the criterion $\hat{f} = 1/2$ for quantum chaos, we applied the Fano factor method to some emblematic ensembles of the RMT. We generated ensembles of ten random matrices of dimension 2000×2000 for the following symmetries: Gaussian diagonal (GDE) and Gaussian orthogonal (GOE) ensembles. The distributions of nearest-neighbor energy level spacings of GDE and GOE correspond with the Poisson limit and the chaotic limit, respectively.

Applying Eq. (1) to the two ensembles, we obtain the following results. For the GDE ensemble, using ten matrices, we obtained the value $\hat{f}_{GDE} = 1.004 \pm 0.003$, which corresponds to the Poisson limit. For the GOE ensemble we found $\hat{f}_{GOE} = 0.54 \pm 0.01$, which confirms our conjecture that it corresponds to quantum chaos.

V. CONCLUSION

We have shown that quantum chaos behavior in nuclear physics using the definition of the Fano factor is consistent with the theory of electronic transport (ballistic billiards), RMT and other surmises such as Wigner and Poisson densities, and the Fourier power spectrum method; therefore we can speculate that $\hat{f} = 1/2$ can represent another criterion to measure quantum chaos in atomic nuclei. Maybe in the future we can obtain a more complete theory where the Fano factor will depend in the interaction parameter χ. The result presented in this article could be important for other areas of science where the Fano factor is commonly used and do not know how interpret Fano factor values lower than 1.

ACKNOWLEDGMENTS

We acknowledge financial support from PAPIIT-UNAM-IN116716, PAPIME-UNAM-PE111319, and the Red de Tecnologías Cuánticas, CONACyT.

[1] O. Bohigas, M. J. Giannoni, and C. Schmit, Characterization of Chaotic Quantum Spectra and Universality of Level Fluctuation Laws, Phys. Rev. Lett. **52**, 1 (1984).

[2] M. Berry, Quantum chaology (The Bakerian Lecture, 1987), Proc. R. Soc. London A **413**, 183 (1987).

[3] M. C. Gutzwiller, *Chaos in Classical and Quantum Mechanics*, Interdisciplinary Applied Mathematics Vol. 1 (Springer, New York, 1990).

[4] B. V. Chirikov, F. M. Izraelev, and D. L. Shepelyansky, Dynamical stochasticity in classical and quantum mechanics, Sov. Sci. Rev. C **2**, 209 (1981); *Decoherence and the Appearance of a Classical World in Quantum Theory* (Springer, Berlin, 2003).

[5] E. P. Wigner, Random Matrices in Physics, SIAM Rev. **9**, 1 (1967).

[6] M. L. Mehta, *Lectures on Random Matrices and Applications*, 3rd ed. (Elsevier, Amsterdam, 2004).

[7] F. J. Dyson, Statistical theory of the energy levels of complex systems, I, II, and III, J. Math. Phys. **3**, 140 (1962).

[8] T. A. Brody, J. Flores, J. B. French. P. A. Mello, A. Pandey and S. S. M. Wong, Random-matrix physics: Spectrum and strength fluctuations, Rev. Mod. Phys. **53**, 385 (1981).

[9] A. Relaño, J. M. G. Gómez, R. A. Molina, J. Retamosa, and E. Faleiro, Quantum Chaos and $1/f$ Noise, Phys. Rev. Lett. **89**, 244102 (2002).

[10] E. Faleiro, J. M. G. Gómez, R. A. Molina, L. Muñoz, A. Relaño, and J. Retamosa, Theoretical Derivation of $1/f$ Noise in Quantum Chaos, Phys. Rev. Lett. **93**, 244101 (2004).

[11] E. Landa, Irving O. Morales, R. Fossion, P. Stránský, V. Velázquez, J. C. López Vieyra, and A. Frank, Criticality and long-range correlations in time series in classical and quantum systems, Phys. Rev. E **84**, 016224 (2011).

[12] U. Fano, Ionization yield of radiations. II. The fluctuations of the number of ions, Phys. Rev. **72**, 26 (1947).

[13] K. Rajdl and P. Lansky, Shot-noise Fano factor, Phys. Rev. E **92**, 052135 (2015).

[14] M. Blanter and M. Bioettiker, Shot noise in mesoscopic conductors, Phys. Rep. **336**, 1 (2000).

[15] F. Farkhooi, M. F. Strube-Bloss, and M. P. Nawrot, Serial correlation in neural spike trains: Experimental evidence, stochastic modeling, and single neuron variability, Phys. Rev. E **79**, 021905 (2009).

[16] M. P. Nawrot, C. Boucsein, V. R. Molina, A. Riehle, A. Aertsen, and S. Rotter, Measurement of variability dynamics in cortical spike trains, J. Neurosci. Methods **169**, 374 (2008).

[17] L. Telesca and L. Toth, Analysis of temporal fluctuations in the 1880–1994 seismicity of Pannonian Basin, Fluct. Noise Lett. **09**, 157 (2010).

[18] A. C. Barato and U. Seifert, Universal bound on the Fano factor in enzyme kinetics, J. Phys. Chem. B **119**, 6555 (2015).

[19] M. Fox, *Quantum Optics: An Introduction* (Oxford University Press, Oxford, 2006).

[20] C. W. J. Beenakker and M. Büttiker, Suppression of shot noise in metallic diffusive conductors, Phys. Rev. B **46**, 1889 (1992).

[21] R. A. Jalaber, J.-L. Pichard and C. W. J. Beenakker, Universal quantum signatures of chaos in ballistic transport, Europhys. Lett. **27**, 255 (1994).

[22] O. Agam, I. Aleiner, and A. Larkin, Shot Noise in Chaotic Systems: Classical to Quantum Crossover, Phys. Rev. Lett. **85**, 3153 (2000).

[23] Robert S. Whitney and Ph. Jacquod, Shot Noise in Semiclassical Chaotic Cavities, Phys. Rev. Lett. **96**, 206804 (2006).

[24] S. Oberholzer, E. V. Sukhorukov, and C. Schönenberger, Crossover between classical and quantum shot noise in chaotic cavities, Nature (London) **415**, 765 (2002).

[25] Ph. Jacquod and R. S. Whitney, Semiclassical theory of quantum chaotic transport: Phase-space splitting, coherent backscattering, and weak localization, Phys. Rev. B **73**, 195115 (2006).

[26] E. Caurier and F. Nowacki, Present status of shell model techniques, Acta Physica Polonica, Series B **30**, 705 (1999).

[27] J. Retamosa, variation of ANTOINE for schematic models, 1990 (unpublished).

[28] M. Dufour and A. P. Zuker, Realistic collective nuclear Hamiltonian, Phys. Rev. C **54**, 1641 (1996).

[29] E. Caurier, G. Martínez-Pinedo, F. Nowacki, A. Poves, and A. P. Zuker, The shell model as a unified view of nuclear structure, Rev. Mod. Phys. **77**, 427 (2005).

[30] R. U. Haq, Density and fluctuations in shell model spectra, Pramana J. Phys. **32**, 457 (1989).